

Faster and safer evacuations induced by closed vestibules

I.M. Sticco^a, G.A. Frank^b, C.O. Dorso^{a,c},

^a*Universidad de Buenos Aires, Facultad de Ciencias Exactas y Naturales, Departamento de Física, Buenos Aires, Argentina.*

^b*Unidad de Investigación y Desarrollo de las Ingenierías, Universidad Tecnológica Nacional, Facultad Regional Buenos Aires, Av. Medrano 951, 1179 Buenos Aires, Argentina.*

^c*CONICET-Universidad de Buenos Aires, IFIBA, Buenos Aires, Argentina.*

Abstract

Improving emergency evacuations is a top priority in human safety and in pedestrian dynamics. In this paper, we use the social force model, in order to optimize high-anxiety pedestrian evacuations. We explore two architectural layouts, the 1-door vestibule, and the 2-doors vestibule. The “vestibule” is defined as the room next to the exit door and it is characterized by two structural parameters: the vestibule width (d) and the vestibule door width (w). We found that, specific values of d and w , can almost double the evacuation flow compared to the no-vestibule scenario. The key to this achievement is that the density (close to the exit door) can be controlled by d and w . Therefore, it is possible to tune these parameters to a density that maximizes the available space while preventing the formation of blocking clusters at the exit door ($\rho \sim 2.5 \text{ p/m}^2$). As opposed to the optimal condition, low-density values ($\rho \sim 1 \text{ p/m}^2$) lead to suboptimal flow since there is unused space left; while higher density values ($\rho \sim 4 \text{ p/m}^2$) also lead to suboptimal flow due to the presence of blocking clusters at the exit. Moreover, we take into account the usually foreseen fact that high pressures can actually be reached at the exit, threatening the health of pedestrians. Therefore, we studied the crowd pressure using the agents’ overlap as an indicative. We found that the explored vestibules reduce the crowd pressure compared to the no-vestibule situation. In particular, we show that the 2-doors vestibule scenario performs better than the 1-door vestibule, because it

reduces the overall local density (by enforcing the crowd to spread out more).

Keywords: Pedestrian evacuation, obstacle, vestibule, social force model.

1. Introduction

Improving emergency evacuations is an issue of fundamental importance for human safety. Despite the efforts being done by crowd management legislations worldwide, catastrophic events such as human stampedes and fatal emergency evacuations are still common [1, 2]. In the last years, the scientific community has arrived at a growing number of ideas to address this problem [3, 4]. The proposed solutions can be classified into three categories [5]: planning-based solutions, behavioral-based solutions and architectural-based solutions.

In the first place, planning-based solutions consist of optimizing the departure schedule and planning the right path to escape a building [6, 7]. Sometimes these solutions require a central authority to control the crowd. Secondly, behavioral-based solutions consist of proposing modifications in the attitude of the pedestrians [8, 9]. These solutions require training and proper instructions to be acquired by potential evacuating individuals.

Finally, architectural-based solutions consist of proposing design and infrastructure adjustments that reduce the evacuation time and increase safety during the evacuation process. Unlike the aforementioned approaches, the architectural-based solutions do not focus on the guidance of pedestrians nor their specific training.

Among the three approaches, the most popular one is the architectural-based. In particular, positioning an exit in the corner of a room [10] and placing an obstacle in front of the exit door [11] appear to reduce the evacuation time in both numerical simulations [12, 13], and controlled experiments [14].

In the seminal work of Helbing et al., it was proposed for the first time the use of a column-like obstacle to improve the evacuation performance [3]. Since then, many efforts have been made to understand this phenomenon. Although some results favor the initial hypothesis [11], some others challenge the statement that the column-like obstacle can enhance the evacuation performance [15].

Placing panel-like obstacles instead of pillar-like obstacles, although it is a simpler proposal, it appears as a more promising solution in terms of increasing the evacuation flow. There are numerical results [12] as well as experimental evidence [14] that support this idea.

The authors in Ref. [13] postulate the idea that placing two panel-like obstacles in front of the exit door improves the evacuation performance. They introduce the concept of “vestibule” (say, the space near the exit door) as a more relevant one than the obstacle itself. The authors found that the evacuation flow is determined by the density at the vestibule. Moreover, the density can be controlled by architectural features such as the number of vestibule doors, the vestibule width and the wall friction coefficient.

In addition to improving the evacuation flow, it is important to reduce the physical pressure exerted on individuals. Many different approaches appeared in the literature regarding the pressure in crowd dynamics [16]. The pressure used in some empirical and experimental studies is defined as the product of the local density and the velocity variance [17]. This magnitude has proved to correlate with the probability of tripping and the anxiety level [18].

Other approach worth mentioning is the numerical study done by Cornes et al. which define pressure as a function of the normal forces acting on the individuals [19]. In line with this, it is worth remarking the experimental efforts done by different authors who craft “pressure vests” in order to measure the contact forces applied to the human thorax [20].

This paper is a numerical study that is framed in the architectural-based approach. We investigate emergency evacuations in the presence of a closed vestibule. The closed vestibule is defined as the room next to the exit door which is enclosed by panel-like obstacles. We show that this layout is capable of improving emergency evacuations for two reasons. On one hand, it substantially increases the evacuation flow of pedestrians. On the other hand, it reduces the pressure exerted on them.

The paper is organized as follows. In Section 2, we present the model and theoretical definitions. In section 3, we describe the numerical simulations and the explored layouts. The results are exhibited in Section 4. We finally resume the conclusions in Section 5.

2. Background

2.1. The Social Force Model

The social force model [3] provides the necessary framework for simulating the collective dynamics of pedestrians (*i.e.* self-driven agents). The pedestrians are represented as moving particles that evolve according to the presence of either “socio-psychological” forces and physical forces. The equation of motion for any agent i of mass m_i reads

$$m_i \frac{d\mathbf{v}_i}{dt} = \mathbf{f}_d^{(i)} + \sum_{j=1}^N \mathbf{f}_s^{(ij)} + \sum_{j=1}^N \mathbf{f}_p^{(ij)} \quad (1)$$

where the subscript j corresponds to any neighboring agent or the walls. The three forces \mathbf{f}_d , \mathbf{f}_s and \mathbf{f}_p are different in nature. The desire force \mathbf{f}_d represents the acceleration of a pedestrian due to his/her own will. The social force \mathbf{f}_s , instead, describes the tendency of the pedestrians to stay away from each other. The physical force \mathbf{f}_p stands for both the sliding friction and the repulsive body force.

The pedestrians' own will is modeled by the desire force \mathbf{f}_d . This force stands for the acceleration required to move at the desired walking speed v_d . For a fixed parameter τ reflecting the reaction time, the desire force is modeled as follows

$$\mathbf{f}_d^{(i)} = m \frac{v_d^{(i)} \hat{\mathbf{e}}_d^{(i)}(t) - \mathbf{v}^{(i)}(t)}{\tau} \quad (2)$$

where $\hat{\mathbf{e}}(t)$ represents the unit vector pointing to the target position and $\mathbf{v}(t)$ stands for the agent velocity at time t .

The tendency of any individual to preserve his/her personal space is accomplished by the social force \mathbf{f}_s . This force is expected to prevent the agents from getting too close to each other (or to the walls) in any usual environment. The model for this kind of ‘‘socio-psychological’’ behavior is as follows

$$\mathbf{f}_s^{(i)} = A e^{(R_{ij}-r_{ij})/B} \hat{\mathbf{n}}_{ij} \quad (3)$$

where r_{ij} is the distance between the centers of mass of particles i and j , and $R_{ij} = R_i + R_j$ is the sum of the pedestrians radius. The unit vector $\hat{\mathbf{n}}_{ij}$ points from pedestrian j to pedestrian i , meaning a repulsive interaction. The parameter B is a characteristic scale that plays the role of a fall-off length within the social repulsion. At the same time, the parameter A represents the intensity of the social repulsion.

The expression for the physical force (the friction force plus the body force) has been inspired from the granular matter field [21]. The mathematical expression reads as follows

$$\mathbf{f}_p^{(ij)} = \kappa_t g(R_{ij} - r_{ij}) (\Delta \mathbf{v}^{(ij)} \cdot \hat{\mathbf{t}}_{ij}) \hat{\mathbf{t}}_{ij} + k_n g(R_{ij} - r_{ij}) \hat{\mathbf{n}}_{ij} \quad (4)$$

where $g(R_{ij} - r_{ij})$ equals $R_{ij} - r_{ij}$ if $R_{ij} > r_{ij}$ and vanishes otherwise. $\Delta \mathbf{v}^{(ij)} \cdot \hat{\mathbf{t}}_{ij}$ represents the relative tangential velocities of the sliding bodies (or between the pedestrian and the walls).

The sliding friction occurs in the tangential direction while the body force occurs in the normal direction. Both are assumed to be linear with respect to the net distance between contacting agents. The sliding friction is also linearly related to the difference between the tangential velocities.

The coefficients κ_t (for the sliding friction) and k_n (for the body force) are related to the contacting surface materials and the body stiffness, respectively. The friction force between an agent and a wall/panel has the same mathematical expression as the friction between two agents.

The model parameter values were chosen to be the same as the best-fitting parameters reported in the recent study from [22]. These values were obtained by fitting the model to a real-life event that resembles an emergency evacuation. The parameter values are: $A = 2000 \text{ N}$, $B = 0.08 \text{ m}$, $\kappa_t = 3.05 \times 10^5 \text{ kg/(m.s)}$, $k_n = 3600 \text{ N/m}$, $\tau = 0.5 \text{ s}$.

2.2. Blocking clusters

A characteristic feature of pedestrian dynamics is the formation of clusters. Clusters of pedestrians can be defined as the set of individuals that for any member of the group (say, i) there exists at least another member belonging to the same group (j) in contact with the former. Thus, we define a “granular cluster” (C_g) following the mathematical formula given in [23]

$$C_g : P_i \in C_g \Leftrightarrow \exists j \in C_g / r_{ij} < (R_i + R_j) \quad (5)$$

where (P_i) indicate the i th pedestrian and R_i is his/her radius (half of the shoulder-to-shoulder width). That means, C_g is a set of pedestrians that interact not only with the social force, but also with physical forces (*i.e.* friction force and body force). A “blocking cluster” is defined as the minimal granular cluster which is closest to the door whose first and last agents are in contact with the walls at both sides of the door (*i.e.* the first and last agents are the closest

ones to each doorjamb) [24]. Previous studies demonstrated that the blocking clusters play a crucial role in preventing pedestrians from getting through a door [24, 25, 26].

3. Numerical simulations

We performed numerical simulations of pedestrians evacuating a room in the presence of a 1-door vestibule and a 2-doors vestibule (see Fig. 1 and Fig. 2, respectively). We simulated crowds of $N=200$ agents whose trajectories followed the equation of motion (1). We used the circular specification of the social force model for the interaction forces acting on the agents (see Section 2.1 for the corresponding mathematical expressions). The model parameter values were chosen to be the same as the best-fitting parameters reported in the recent study [22], and the ones cited in Section 2.1.

The mass of the agents was fixed at $m = 80$ kg, and the radius was set to $R = 0.23$ m according to data reported in [27]. The desired velocity (which is the parameter that controls the anxiety level) was varied in the interval $1 \text{ m/s} \leq v_d \leq 6 \text{ m/s}$. Although the upper limit ($v_d = 6 \text{ m/s}$) may seem rather extreme, recent empirical measurements at San Fermín bull-running festival in Pamplona shows that non-professional runners can achieve velocities $v \sim 6 \text{ m/s}$ [28].

Initially, the agents are placed in a $20 \text{ m} \times 20 \text{ m}$ area with random positions and velocities. The direction of the desired velocity was such that the agents located outside the vestibule point to the nearest vestibule door. Once they are inside the vestibule, the updated target becomes the exit door.

The exit door’s size was $DS = 1.84 \text{ m}$, which is equivalent to four agents’ diameter in accordance to [22]. The 1-door vestibule (Fig. 1) is composed of 2 panel-like obstacles (*i.e.* walls). The walls that define the vestibule extend to the side of the room. The door of the vestibule is placed symmetrically with

respect to the exit door. The width of the vestibule door is w . See Section 3.1 for more details.

The 2-doors vestibule layout (Fig. 2) is composed of 3 panel-like obstacles. At this instance, we chose a commonly expected configuration: the middle panel shares the same length as the exit door DS , and it is placed right in front of it. The left and right panels are as long as the room. Both vestibule doors have the same width $w/2$ (therefore, the total vestibule entry width is w). The middle panel is fixed (in length and location) regardless of w . This means that increasing w widens each door outwards.

In this research, we analyzed the effect of varying 3 parameters: the desired velocity v_d , the vestibule width d , and the total vestibule door width w . For each parameter configuration, we performed 30 evacuation processes that finished when 90% of agents left the room. No re-entry of agents was allowed.

We recorded the positions and velocities every 0.5 s from the beginning of the simulation until the end (*i.e.* when 90% of the individuals have left the room). Then, we computed the mean density, the evacuation flow, and the probability of blocking clusters formation.

The density was measured in the inner vestibule region and it was defined as the number of pedestrians divided by the inner vestibule area (see Fig.1 and Fig.2). The area of the inner vestibule is $DS \times d$ (where DS stands for the size of the exit door and d is the vestibule width). The density was calculated every 0.5s. Afterward, the mean and standard deviation were computed from the recorded values.

The evacuation flow is defined as follows,

$$J = \frac{n}{t_e} \quad (6)$$

where n is the number of evacuated pedestrians and t_e is the time it takes for those pedestrians to evacuate the room. The evacuation finished when 90% of the initial number of pedestrians abandoned the room.

The blocking clusters are the set of pedestrians that block a door (see Section 2.2 for a formal definition). We measured the probability of blocking clusters formation in three different regions: the exit door, the doors of the vestibule, and also the blocking clusters inside the vestibule. The probability is defined as the fraction of time that the blocking clusters are formed over the total evacuation time.

The numerical simulations were carried out using LAMMPS, which is a molecular dynamics open-access software [29]. The implementation also required customized modules developed in C++. The integration of the agents' trajectory was computed using the Velocity Verlet algorithm with a time-step $\Delta t = 10^{-4}$ s.

3.1. The explored layouts

In architecture, a vestibule is defined as a small room that leads to a larger space [30]. In this paper, we consider vestibules placed next to the exit door. Two different layouts were explored: the 1-door vestibule and the 2-doors vestibule. Fig. 1 illustrates the 1-door vestibule layout. It consists of 4 walls in total. Two walls delimit the exit door and, the other two delimit the vestibule door.

The vestibule is a corridor as long as the room and width d . It has a single door of width w in front of the exit door. The shady area in Fig. 1 represents

the “inner vestibule”, which we define as the rectangular area enclosed by the exit door and the vestibule door (this area will be relevant in our analysis).

1-door vestibule

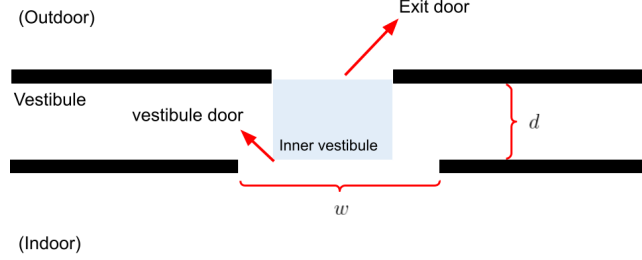


Figure 1: 1-door vestibule layout. The vestibule door of width w is placed in front of the exit door. The vestibule looks like a corridor as long as the room and width d . The sides of the room are not drawn.

The 2-doors vestibule layout is exhibited in Fig. 2. In this case, each vestibule door has a width $w/2$ (w is the total vestibule door size). The two doors are separated by a wall similar in size to the exit door. This wall is located in front of the exit door. The 2 vestibule doors are symmetrically located with respect to the exit. The shady area in Fig. 2 represents the inner vestibule. In this case, it is defined as the rectangular area enclosed by the exit door and the opposing wall.

Notice that, we are dealing only with “closed vestibules” rather than “open vestibules”. These are closed vestibules since the enclosing walls are as wide as the room. On the other hand, the open vestibules are characterized by one (or multiple) panel-like obstacles in front of the exit door. Previous research dealt with open vestibules where pedestrians were able to dodge the obstacles [13] or even step over them [31] in order to access the vestibule. Instead, in the closed vestibule scenario, pedestrians have to go through the vestibule doors to access

2-doors vestibule

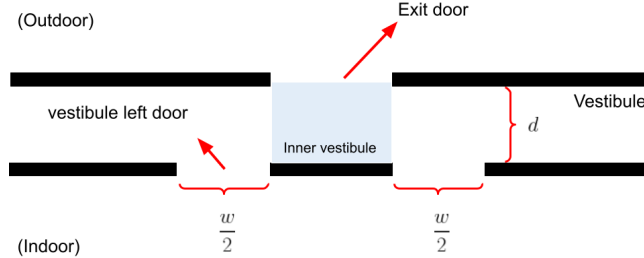


Figure 2: 2-doors vestibule layout. $w/2$ is the width of each vestibule door. Both vestibule doors are symmetrically placed in front of the exit door. The vestibule is a corridor as long as the room and width d . The sides of the room are not drawn.

it.

3.2. Clarifications

We will refer to d (the vestibule width) and w (the vestibule door width) as the “structural parameters”. In order to keep a clear notation, we will express the structural parameters (d and w) in units of the agent’s diameter. For example, if $w = 4$, we actually mean that $w = 4 \times 0.46 \text{ m} = 1.84 \text{ m}$. Where 0.46 m is the average pedestrian’s shoulder-to-shoulder distance reported in [27].

Regarding the panel-like obstacles that define the vestibule, these panels reach the sides of the room. Therefore, individuals can’t dodge them. Moreover, in this research, panel-like obstacles are treated as walls (meaning that individual-panel interactions are the same as the individual-wall interaction).

In this research, we use the agents’ overlap as a reasonable indicator for the pressure exerted on them. We are aware that the overlap does not have units of pressure. Nevertheless, we argue that any reasonable measure of pressure should be correlated with the overlap since all the forces acting in the normal

direction are monotonically non-decreasing functions of the overlap. In Section 4.3, we will use the term “overlap” as a synonym of “pressure”.

Throughout this paper, we use the symbol ρ to denote the density in the inner vestibule region. In the same way, we use the symbol J to refer to the evacuation flow.

4. Results and discussions

This Section is divided into three parts. In the first part (Section 4.1), we show the results corresponding to the 1-door vestibule layout for $N=200$. The second part corresponds to the 2-doors vestibule layout (Section 4.2). These two sub-sections focus on the evacuation flow improvement that is possible to achieve with the aforementioned layouts. The explanation for this improvement is based on the fundamental diagram and the blocking cluster probability (also discussed in the aforementioned Sections).

Finally, in Section 4.3 we further examine the effects of both vestibule layouts on the crowd pressure. We compare one layout against the other and also against the no-vestibule condition.

4.1. The 1-door vestibule

We present in this Section the main results corresponding to the 1-door vestibule layout that was previously introduced in Fig. 1. We explore a wide range of values for the structural parameters d and w and its consequences on the evacuation flow. Under some structural conditions, the presence of a 1-door vestibule improves the evacuation. At the end of the Section, we provide an explanation of the flow improvement given by the relation between the density inside the vestibule and the blocking clusters.

Fig. 3 shows the evacuation flow as a function of the vestibule door size (w) for different vestibule widths (d). The evacuation flow is defined in Eq. (6). The horizontal dashed line in Fig. 3 stands for the “no-vestibule” situation. If a curve surpasses the horizontal dashed line, it means that the vestibule yields an enhanced evacuation flow with respect to the no-vestibule situation. Each plot corresponds to a different desired velocity v_d as indicated in the plot’s titles.

If w is small ($w \leq 4$), the evacuation flow of the vestibule situation is equal to (or less than) the no-vestibule situation. On the opposite limit ($w > 10$), the evacuation flow also converges to the no-vestibule situation. Notably, intermediate w values yield an evacuation flow that is much higher than the no-vestibule situation. This behavior holds for any v_d in the range $2.5 \text{ m/s} \leq v_d \leq 6 \text{ m/s}$. Fig. 3a and Fig. 3b show the results corresponding to $v_d = 3 \text{ m/s}$ and $v_d = 6 \text{ m/s}$, respectively.

Notice that, regardless of v_d , varying d does not affect the qualitative behavior of the flow curves. However, the evacuation flow strongly depends on w . Therefore, in the 1-door vestibule, we can assure that the evacuation flow is dominated by the structural parameter w rather than d .

The largest difference between the 1-door vestibule situation and the no-vestibule scenario is given in $d = 4$, $w = 6$ and $v_d = 6 \text{ m/s}$. In this case, the flow increment is more than 4 p/s (which represents a 70 % increment). In a real-life environment, such a big contrast might be the difference between a regular evacuation and a disastrous event.

At a first inspection, the flow increment provided by the vestibule can be explained by the density in the “inner vestibule”.

Recall that, the fundamental diagram (flow-density plot) is a meaningful chart for the “free-flow” regime (where the flow increases as the density in-

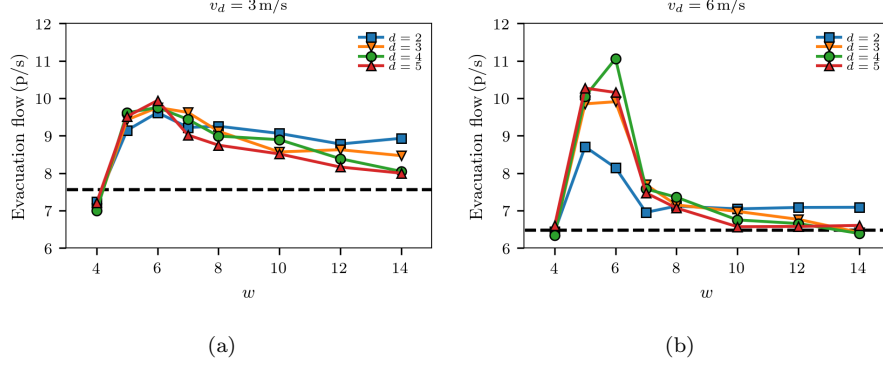


Figure 3: Evacuation flow as a function of the vestibule door width w for 1-door vestibules. Each curve corresponds to a different vestibule width d . The horizontal dashed line indicates the flow for the “no-vestibule” scenario. Data was averaged over 30 evacuation processes with random initial positions and velocities. The initial number of pedestrians was $N=200$. **(a)** the desired velocity was $v_d = 3$ m/s, **(b)** the desired velocity was $v_d = 6$ m/s.

creases) and the “congested” regime (where the flow diminishes as the density increases). The former is associated with a low-density scenario, whereas the latter is associated with a high-density scenario.

Fig. 4a exhibits the fundamental diagram for the 1-door vestibule at $d = 4$ and $v_d = 6$ m/s. The horizontal dashed line corresponds to the no-vestibule situation. The markers stand for the w values and the solid curve is the average over the data points. The data points correspond to different initial conditions.

The lowest w values yield a free-flow regime, while the largest w produce a congested regime. Notice that $w = 6$ is the door width for intermediate densities ($\rho \sim 2.5$ p/m²) and the maximum evacuation flow. We will explain the details of this phenomenon at the end of this Section.

If the density on the inner vestibule is low (say, $\rho \sim 1$ p/m²), the evacuation flow is below the optimal condition because there is unused space left close to

the exit door. This phenomenon makes the crowd to evacuate “in dribs and drabs”.

If the density is high ($\rho \sim 4 \text{ p/m}^2$), the evacuation flow is also suboptimal because the area close to the exit door gets congested and produces blocking clusters that hinder the flow.

However, the intermediate density values ($\rho \sim 2.5 \text{ p/m}^2$) trade-off the two above mentioned phenomenons and therefore maximize the evacuation flow.

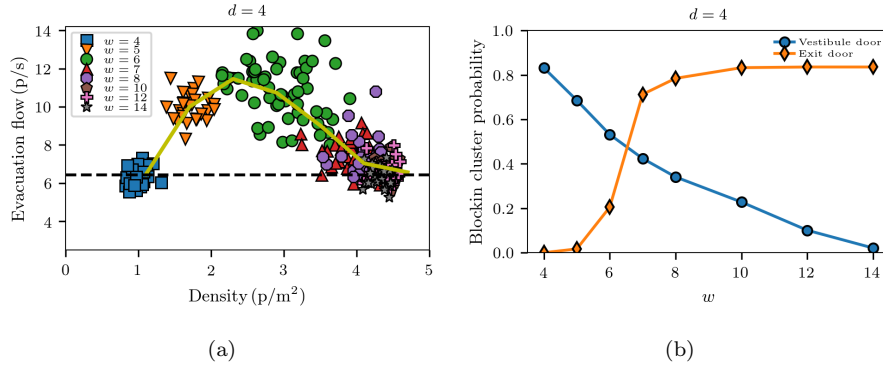


Figure 4: **(a)** Evacuation flow as a function of the density (fundamental diagram) for 1-door vestibules. The horizontal dashed line indicates the flow for the “no-vestibule” scenario. The density was measured on the inner vestibule and, it was averaged until 90% of individuals evacuated. Each data point belongs to a single evacuation process where the initial condition (positions and velocities) were set to random. **(b)** Blocking cluster probability as a function of the vestibule door width w . The probability is defined as the fraction of time that a blocking cluster is present over the total evacuation time. The initial number of pedestrians was $N=200$. The desired velocity was $v_d = 6 \text{ m/s}$.

To complete the picture, we calculated the blocking cluster probability at the exit door and also at the vestibule door. A blocking cluster is defined as the set of pedestrians in physical contact that clog a door. Previous studies have shown that blocking clusters play a critical role in high-anxiety evacuation

processes [24, 26].

Fig. 4b shows the blocking cluster probability as a function of the vestibule door size w . Recall that, the blocking cluster probability is defined as the fraction of time that a blocking cluster is present over the total evacuation time.

The vestibule door curve and the exit door curve display an anti-correlation pattern (see Fig. 4b). If the vestibule door is small ($w \leq 6$), there is a high blocking cluster probability at the vestibule door. The blocking clusters at the vestibule door prevent the inner vestibule from having high densities. This is why, for small w , the presence of blocking clusters at the exit door is almost negligible (< 0.2).

Increasing w reduces the blocking clusters at the vestibule door, letting a larger number of pedestrians access the inner vestibule at the same time. As a consequence, the exit door blocking cluster probability exhibits a sharp increase at $w = 7$. Notice that, this increment is in agreement with the flow reduction of the congested regime exhibited at the fundamental diagram (see Fig. 4a).

It is worth clarifying that, although we only show the fundamental diagram and the blocking clusters corresponding to $d = 4$, the qualitative behavior at different d values is similar. In the same way, despite we only exhibit results for $v_d = 3$ m/s and $v_d = 6$ m/s, the qualitative behavior of the results for any desired velocity in the interval $v_d \geq 2.5$ m/s is similar to the ones presented here.

To conclude the Section, we remark that the evacuation flow is sensible to the inner vestibule density. At the same time, this density can be controlled mainly by the structural parameter w . Our most important result is that the evacuation flow gets maximized when the inner vestibule achieves a maximum density value such that almost no blocking clusters are produced at the exit door but not as low as to evacuate “in dribs and drabs”.

4.2. The 2-doors vestibule

In this Section, we present the results corresponding to the 2-doors vestibule layout (illustrated in Fig. 2). This Section is organized in a similar fashion to the previous one. First, we explore the structural parameters (d and w) that improve the evacuation flow and its relation to the fundamental diagram. Then, we discuss about the blocking clusters’ role in relation to the fundamental diagram and the evacuation performance.

The evacuation flow as a function of the vestibule’s total door size (w) is shown in Fig. 5. Since we are dealing with 2-doors vestibules, w now stands for the sum of both vestibule door sizes. Recall that in this paper we only explore symmetrical vestibules. That is, the size of each door is $w/2$.

Fig. 5a corresponds to $v_d = 3$ m/s, while Fig. 5b corresponds to $v_d = 6$ m/s. Each curve stands for a different d value (see legends for details). The no-vestibule evacuation flow is shown by the horizontal dashed line. As a first inspection, we can notice that $d = 2$ worsens the evacuation performance, but $d = 3$ increases the evacuation flow until reaching a plateau above the no-vestibule situation.

In the case of $v_d = 3$ m/s (Fig. 5a), the widest vestibules ($d = 4$ and $d = 5$) exhibit similar patterns. Small w values worsen the evacuation performance but, the evacuation flow improves for $w \geq 6$. In both cases, the curves reach a maximum at $w = 8$ and then reduce the flow as w increases.

In the case of $v_d = 6$ m/s (Fig. 5b), the vestibule of size $d = 4$ produces the maximum flow at $w = 8$ (the reader may watch the video in the supplementary material). After this “peak”, the flow slowly diminishes for increasing values of w . It is worth noting that, for $w > 6$, the evacuation flow is substantially higher

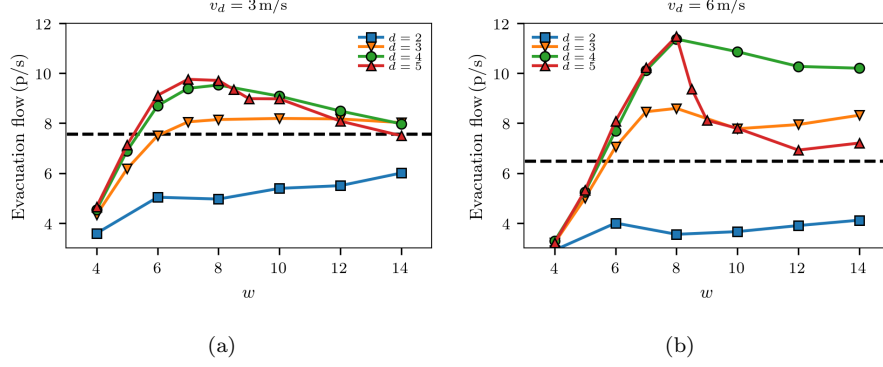


Figure 5: Evacuation flow as a function of the total vestibule door width w for 2-doors vestibules. Each curve corresponds to a different vestibule width d . The horizontal dashed line indicates the flow for the “no-vestibule” scenario. Data was averaged over 30 evacuation processes where the initial positions and velocities were set to random. The initial number of pedestrians was $N=200$. **(a)** the desired velocity was $v_d = 3 \text{ m/s}$, **(b)** the desired velocity was $v_d = 6 \text{ m/s}$.

than the no-vestibule situation.

If the vestibule is wider ($d = 5$) and $v_d = 6 \text{ m/s}$ (see Fig. 5b), the curve also exhibits an interval in which the evacuation flow is much higher than the no-vestibule situation. The “peak” of flow is around $w = 8$ and the flow converges to the no-vestibule scenario as w increases.

It is important to remark that the 2-doors vestibule is capable of improving the evacuation flow under a wide range of values of the structural parameters (d and w).

Interestingly, the maximum flow value for 2-doors vestibule is around $w = 8$, whereas the maximum flow for the 1-door vestibule is around $w = 6$. It means that a single door of size w yields more flow than 2 doors of size $w/2$. Similar results were reported for two-doors pedestrian evacuation simulations [25] and also for experiments performed with granular media accelerated by the force of

gravity [32]. In Appendix B we provide a brief discussion regarding this topic.

The vestibule improves the evacuation flow if certain structural conditions are met (specific values of d and w). At a first inspection, the flow increment can be explained with the help of the fundamental diagram (*i.e.* the flow vs. density plot). As we did for the 1-door vestibule, we measured the evacuation flow as a function of the density. The density was measured in the “inner vestibule” (the area between the exit door and the vestibule wall; see Section 3.1 for details).

Fig. 6 shows the fundamental diagram for different structural parameters (see the titles and the labels). The horizontal line stands for the no-vestibule situation. The markers represent different vestibule door size w and each data point correspond to a different initial condition.

The narrowest vestibule explored is $d = 2$. Under this condition, the density in the inner vestibule remains very low ($\rho < 1$) regardless of the size of the vestibule door (Fig. 6a). The cause of this phenomenon is that pedestrians get stuck at the entrance of the inner vestibule preventing this zone to have a larger number of pedestrians. The direct consequence of this phenomenon is a lower evacuation flow than that of the situation without a vestibule.

Fig. 6b corresponds to 2-doors vestibule and $d = 3$. Although this structural condition allows a wider range of density and flow, only the free-flow regime is observed. This means that the inner vestibule does not get overcrowded (regardless of w). This phenomenon is related to the blocking clusters produced inside the vestibule, as will be discussed at the end of this Section.

For 2-doors vestibules of size $d = 4$ (Fig. 6c), the free-flow and the “peak” of the fundamental diagram are observed. This means that increasing w increases the density while also increasing the evacuation flow. As in the case of $d = 3$, the inner vestibule does not get overcrowded because the agents get stuck (tem-

porarily) before the inner vestibule region.

If the vestibule is wider ($d = 5$), it is possible to observe the free-flow and the congested regime (Fig. 6d). The former holds for $w < 8$, while the latter appears at $w > 9$. The congested regime is characterized by decreasing flow as the density increases. For such a wide vestibule ($d = 5$), and such a large vestibule door size ($w > 8$), a large number of agents are allowed to enter the vestibule at the same time. This is the limit that resembles the no-vestibule scenario.

To complete the picture of why the inner vestibule gets crowded depending on d and w , we measured the blocking clusters. Unlike the 1-door vestibule, for the 2-doors vestibule, it is necessary to define a new type of blocking cluster: the “inside vestibule blocking cluster”. These are blocking clusters that are formed inside the vestibule but just before the inner vestibule.

In summary, three types of blocking clusters play a relevant role. The ones that are formed at the exit door, the ones that are formed before the vestibule (at the vestibule door), and the ones that are formed inside the vestibule (just before the inner vestibule). See Appendix C for an illustration of the blocking cluster types. In any case, the blocking cluster probability is defined as the fraction of time that blocking clusters are present over the total evacuation time.

Fig. 7a and Fig. 7b show the three types of blocking cluster probabilities for $d = 3$ and $d = 5$, respectively. As expected, increasing w reduces the vestibule door blocking clusters. The main difference between the case for $d = 3$ and $d = 5$ is that, in the former, the “inside vestibule curve” is above the “exit door curve”. On the other hand, for $d = 5$, the “exit door curve” is well above the “inside vestibule curve”.

The blocking cluster curves explain the differences in the fundamental dia-

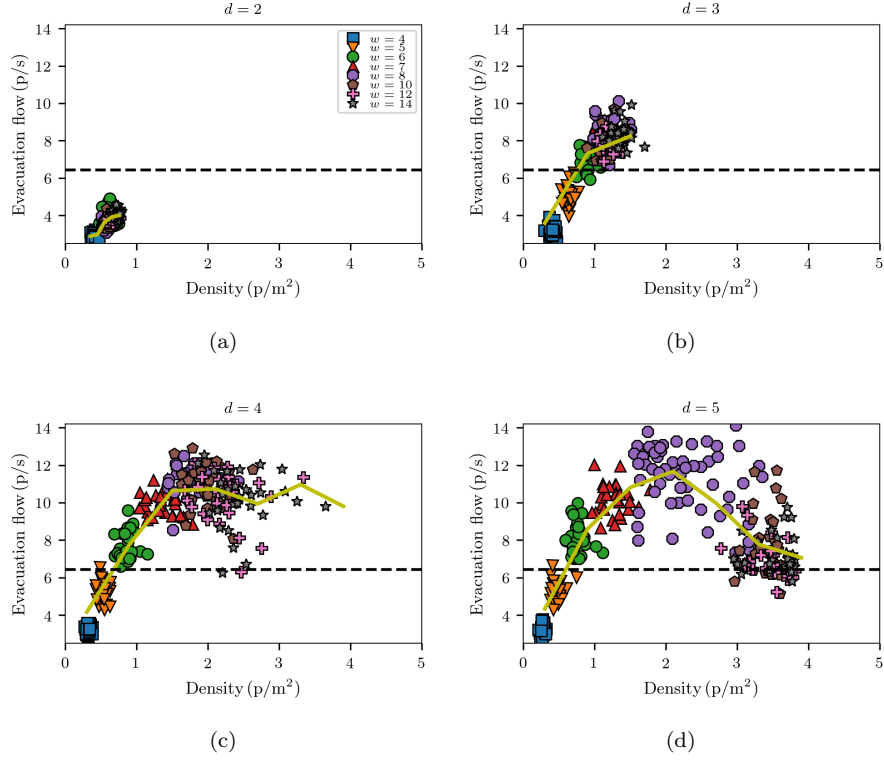


Figure 6: Evacuation flow as a function of the density (fundamental diagram) for 2-doors vestibules. The density was measured on the inner vestibule and, it was averaged until 90% of individuals evacuated. The horizontal dashed line indicates the flow for the “no-vestibule” scenario. Each data point belongs to a single evacuation process where the initial condition (positions and velocities) were set to random. The initial number of pedestrians was $N=200$. The desired velocity was $v_d = 6$ m/s. See the plot’s title for the corresponding value of the vestibule width d .

gram. $d = 3$ increases the blocking cluster probability before the inner vestibule. These blocking clusters prevent the inner vestibule from getting overcrowded. This is why the fundamental diagram at $d = 3$ only exhibits free-flow (and low density). The direct consequence of the low density is the lack of blocking clusters at the exit door. Therefore, the evacuation flow is higher than the no-vestibule condition.

The scenario of $d = 5$ produces fewer blocking clusters before the inner vestibule. Thus, the inner vestibule gets crowded more easily. This is why the fundamental diagram at $d = 5$ exhibits a congested regime (for large enough w). The consequence is an increase in the exit door blocking cluster probability, which reduces the evacuation flow.

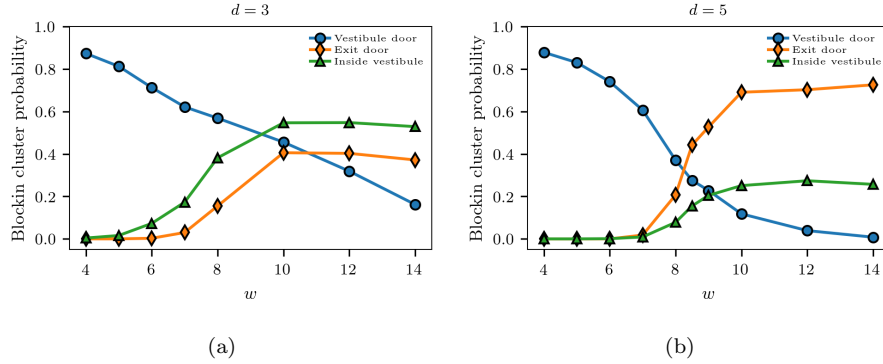


Figure 7: Blocking cluster probability as a function of the vestibule door width w . See the legend for the type of considered blocking cluster. The probability is defined as the fraction of time that a blocking cluster is present over the total evacuation time. The initial number of pedestrians was $N=200$. The desired velocity was $v_d = 6$ m/s. **(a)** For vestibule width $d = 3$, **(b)** For vestibule width $d = 5$.

To conclude this Section, we stress that the evacuation flow in the 2-doors vestibule is strongly dependent on the density. However, it is possible to control the inner vestibule density with the structural parameters d and w . In the same way as the 1-door vestibule, the flow is maximized for intermediate density val-

ues ($\rho \sim 2.5 \text{ p/m}^2$). Under this condition, the density is low enough to minimize the formation of exit door blocking clusters, but not as low as to leave unused space left in the vestibule.

4.3. *The pressure*

In the previous Section, we showed that under certain structural conditions the inclusion of a vestibule at the exit increases the evacuation flow. One concern now is whether the improvement in flow is at the expense of an increase in the pressure suffered by the escaping individuals. This possibility arises because the vestibule is achieved by placing panel-like obstacles and, these obstacles may cause an increase in pressure due to the individual-obstacle interaction. Another arguable matter is whether the vestibule may create higher local density regions where the pressure is maximized.

In this Section, we report the “overlap” between agents as an indicative of the pressure. The overlap on the i -th particle is defined as $o_i = \sum_j [R_{ij} - d_{ij}]$ where $R_{ij} = R_i + R_j$ is the sum of radius of particles i and j . d_{ij} is the distance between mass centers. j stands for any particle (or wall) that is in physical contact with particle i . Thus, the overlap reflects the degree of closeness between pedestrians. We stress that in this Section, we use the terms overlap and pressure interchangeably.

Although the overlap is not the unique way of quantifying the pressure in a crowd [16, 17, 18], we argue that any reasonable measure of pressure should correlate with this magnitude. We support this argument because the forces acting in the normal direction are monotonically non-decreasing functions of the overlap.

Our results show that the presence of a vestibule significantly reduces the pressure on pedestrians. As a first approach, we display 3 snapshots of evacua-

tions for three different layouts: no-vestibule (Fig. 8a), 1-door vestibule (Fig. 8b), and 2-doors vestibule (Fig. 8c). Each circle represents a simulated pedestrian. The color of each agent reflects the level of overlap o_i (see caption for details).

It is easy to observe that the no-vestibule situation exhibits the highest pressure among the three situations explored. The 1-door vestibule produces lower pressure than the no-vestibule situation and, the 2-door vestibule scenario produces even less pressure than the 1-door vestibule (see Fig.8). Two reasons explain the pressure reduction produced by the vestibule, as follows.

The first reason is that the interaction at the vestibule doors reduces the velocity of pedestrians inside the vestibule region (which reduces the pressure). In other words, the vestibule doors alleviate the strain on the escaping pedestrians at the exit. This phenomenon, explains the difference between the no-vestibule scenario and the vestibule condition.

The second reason that explains the pressure reduction concerns crowd dispersion. The more dispersed the crowd is, the lower the pressure. The 2-doors scenario shows a more dispersed crowd in the zone before the vestibule. In other words, the 2-door vestibule “forces the crowd” to split into two halves (one for each door) which produces an overall density reduction (hence a pressure reduction). The parameter w is the key factor to control the crowd dispersion.

We computed the mean overlap to quantify the crowd pressure for different structural conditions (d and w). This metric is the mean crowd overlap averaged over time at different initial conditions. Fig. 9 shows the mean overlap as a function of w for different vestibule widths d . Fig. 9a corresponds to the 1-door vestibule and Fig. 9b corresponds to the 2-doors vestibule. The horizontal dashed line represents the mean overlap for the no-vestibule situation.

For all the explored conditions, the vestibule produces a lower mean overlap

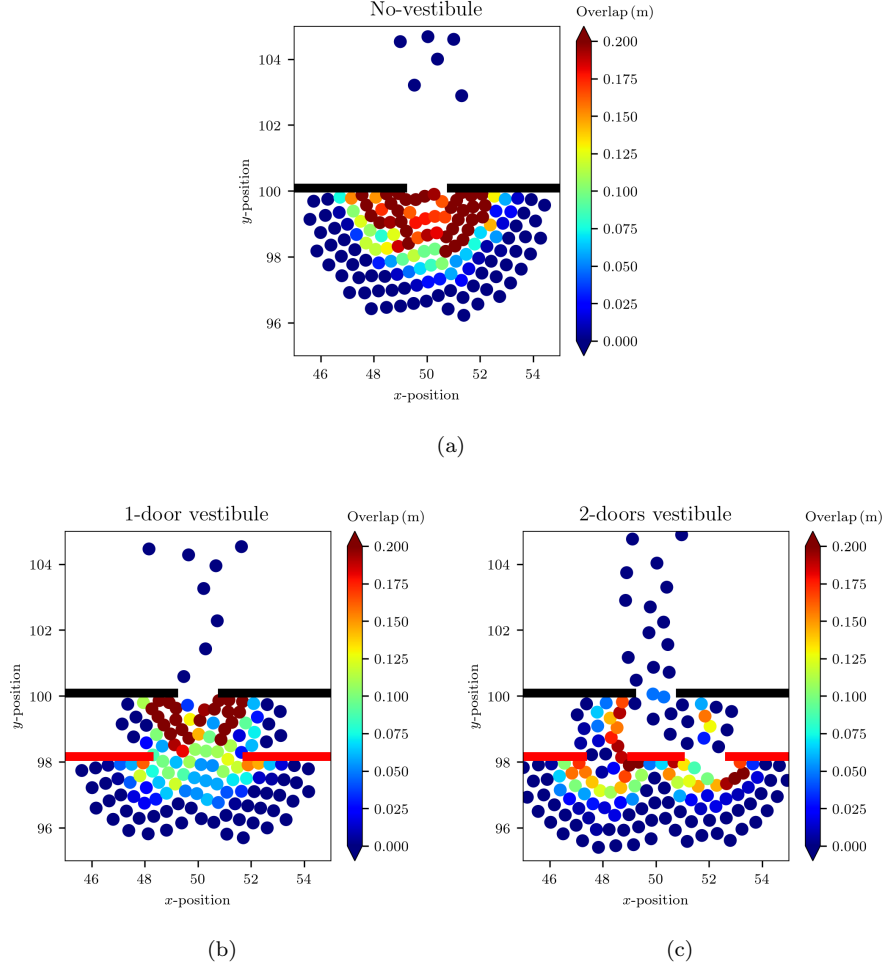


Figure 8: Snapshots of the numerical simulations at $t = 7$ s and $v_d = 6$ m/s. The circles represent the simulated pedestrians. The color on each agent stand for the overlap level (see scale on the right). The title on each plot refers to the layout condition. The 3 scenarios shown begin with the same initial conditions (positions and velocities) for $N=200$ pedestrians. The vestibule door width is $w = 8$ in both cases.

than the no-vestibule situation (all curves lie below the horizontal dashed line in Fig. 9). The 2-door vestibule scenario (Fig. 9b) exhibits less pressure than the 1-door vestibule scenario (Fig. 9a) for any of the structural condition explored. Roughly, the 2-door vestibule shows a decreasing mean overlap as w increases, whereas the 1-door vestibule presents a quasi-constant pattern for any w value.

The decreasing trend in the 2-doors vestibule is a consequence of the crowd dispersion. Recall that, increasing w means increasing the distance between the edges of the 2 doors (see Fig.2). Therefore, in the 2-doors scenario, the higher w , the more spread the crowd is. This phenomenon has a direct consequence on the pressure reduction.

On the other hand, the 1-door vestibule does not significantly spread out the crowd as w increases because the crowd is not split into two halves (unlike in the 2-doors scenario). This is why the overlap exhibits a quasi-constant pattern in Fig. 9a.

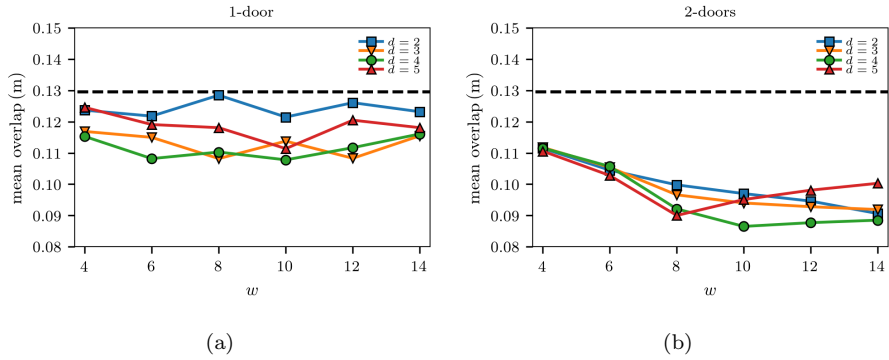


Figure 9: Mean crowd overlap as a function of w for different vestibule widths d . The horizontal dashed line represents the overlap for the no-vestibule situation. The overlap values are averaged over time for 30 different initial conditions. The simulations finished when 180 agents left the room. The initial number of agents was $N=200$ and the desired velocity was $v_d = 6 \text{ m/s}$.

Although the results presented in Fig. 9 correspond to $v_d = 6$ m/s, we obtained similar patterns for desired velocities in the interval $v_d > 2.5$ m/s. We remark that, in addition to the pedestrian-pedestrian interaction, the pedestrian-wall interaction is taken into account in this analysis.

The above results can be summarized as follows. Our numerical simulations indicate that the presence of a vestibule reduces the overall pressure in the crowd. This result holds for any of the structural condition (varying w and d). We highlight that the 2-door vestibule appears as the most effective way of reducing the crowd pressure. The key to this pressure reduction has two components. On one hand, the presence of the vestibule reduces the velocity inside the vestibule region which reduces the pressure. On the other hand, the increase in the parameter w allows the crowd to spread out, thus, reducing the density in the area next to the vestibule.

5. Conclusions

We propose architectural improvements to enhance the evacuation performance in emergency situations. We performed numerical simulations, in the context of the social force model, in order to recreate a crowd of $N=200$ pedestrians evacuating a room under a highly stressing situation ($v_d \geq 3$ m/s).

We explored 3 layout conditions: the no vestibule scenario, the 1-door vestibule, and the 2-doors vestibule. The structural parameters that characterize the vestibule conditions are d (the vestibule width) and w (the vestibule door width). We found that an adequate selection of these parameters can substantially increase the evacuation flow.

The optimal evacuation flow ($J \sim 11$ p/s) is achieved at $d = 4$, $w = 6$ for the 1-door vestibule and, at $d = 4$, $w = 8$ for the 2-doors vestibule. This

is a remarkable improvement considering that the no-vestibule scenario yields $J \sim 6.5 \text{ p/s}$ (for $v_d = 6 \text{ m/s}$ in all cases).

The key to understanding this phenomenon is that d and w control the density in the inner vestibule region. Low density values ($\rho \sim 1 \text{ p/m}^2$) produce a suboptimal evacuation flow because there is unused space left close to the exit door. This state makes the crowd to evacuate “in dribs and drabs”.

Intermediate density values ($\rho \sim 2.5 \text{ p/m}^2$) maximize the evacuation flow because the inner vestibule receives the maximum possible amount of pedestrians without producing many blocking clusters at the exit door. In the opposite case, high density values ($\rho \sim 4 \text{ p/m}^2$), yield a suboptimal evacuation flow because it increases the probability of producing blocking clusters at the exit.

Another important achievement is the pressure reduction attained by the vestibule layouts (in comparison with the no-vestibule scenario). Although both of the explored vestibules (*i.e.* the 1-door and the 2-doors vestibule) reduce the crowd pressure, it is the 2-doors vestibule the one that lowers the pressure the most. This phenomenon occurs because increasing w in this layout forces the crowd to spread out more, thus reducing the local density in the area before the vestibule.

It is also quite relevant that this kind of architectural improvement do not require the pedestrians to be trained to adopt the expected behavior for a successful evacuation.

Although this is a numerical study, we believe that the principles elaborated here are strong enough to be tested empirically in future investigations. As a final word, we would like this paper to be a valuable source of inspiration for future research that truly seeks to improve the human condition.

Appendix A. Evacuation flow for a larger crowd

In order to make a brief assessment of the robustness of the results presented in this paper, we performed numerical simulations for a larger crowd. In this appendix, we show the flow vs. w for different d values for an initial crowd of size $N=600$ (remember that we have already shown results for $N=200$).

Fig. A.10a displays the results corresponding to the 1-door vestibule and Fig. A.10b shows the results corresponding to the 2-doors vestibule. The horizontal dashed line stands for the evacuation flow in the “no-vestibule” scenario at $N=600$. The most remarkable characteristic is that the vestibule still proves to achieve a considerable flow increment for a crowd as large as $N=600$.

Both vestibule layouts seem to improve the evacuation performance. However, the 2-doors vestibule yields higher flow values than the 1-door vestibule. Moreover, in the 2-door vestibule scenario, there is a wider range of structural parameters d and w that surpass the flow of the no-vestibule condition.

The result presented in this appendix suggest that the vestibule improvement can be extrapolated to larger crowds. Nevertheless, we strongly advice exploring the scope and robustness of the vestibule in order to avoid unwanted consequences for the safety of evacuating pedestrians.

Appendix B. Flow vs. door size in the no-vestibule condition

In Section 4 we show the flow vs. w relationships for the 1-door vestibule (Fig. 3) and the 2-doors vestibule (Fig. 5). We noticed that the maximum flow value for the 1-door vestibule is at $w = 6$, whereas the maximum flow value for 2-doors is at $w = 8$. In this appendix, we provide an explanation for this “shifting” behavior.

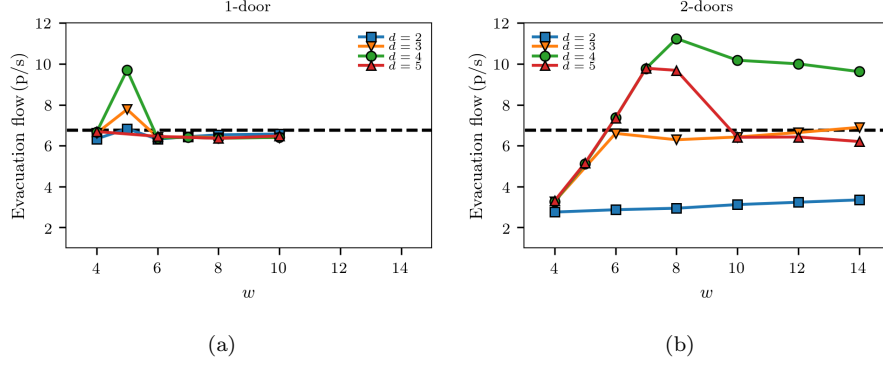


Figure A.10: Evacuation flow as a function of the vestibule door width w . Each curve corresponds to a different vestibule width d . The horizontal dashed line indicates the flow for the “no-vestibule” scenario. Data was averaged over 30 evacuation processes where the initial positions and velocities were random. The initial number of pedestrians was $N=600$. See the plot’s title for the corresponding layout.

First, we calculated the flow vs. w in a regular bottleneck (no-vestibule scenario) to have a more fundamental understanding of the problem. Fig. B.11a show the flow J vs. the door width w for different desired velocities. It is possible to observe 2 distinctive regimes.

The interval $w < 7$ is characterized by the faster-is-slower. This regime is dominated by the blocking clusters and the friction force. On the other hand, the interval $w > 7$ is characterized by the faster-is-faster phenomena (the higher v_d the higher the evacuation flow). In this regime, the door is so large that the blocking clusters become unstable.

We focus on the faster-is-slower regime ($w < 7$) and the desired velocities associated with high anxiety ($v_d \geq 3$ m/s). Therefore, in Fig. B.11b we “zoom in” and show the evacuation flow as a function of w only for $v_d = 6$ m/s. It is worth mentioning that any $v_d \geq 3$ m/s exhibits a similar behavior.

At a first sight, it is possible to observe that the flow does not hold a linear relation in w . This result is in agreement with the laboratory and empirical results reported in Refs. [33, 34]. However, we acknowledge that there is an ongoing discussion on this topic since other experiments seem to yield a linear relation instead of a non-linear one [35, 36].

Nevertheless, the non-linear behavior exhibited in Fig. B.11b is a sufficient justification for the “shifting” behavior in the flow vs. w curves (Fig. 3 and Fig. 5). In other words, the non-linearity in $J(w)$ implies that a layout with only one exit of width w yields more evacuation flow than a layout composed of 2 separated exits of $w/2$ each. If the $J(w)$ was linear, then we would expect no shifting behavior, since in this hypothetical case, the inflow to the vestibule provided by the 1-door scenario would be the same as the 2-doors scenario (at constant w).

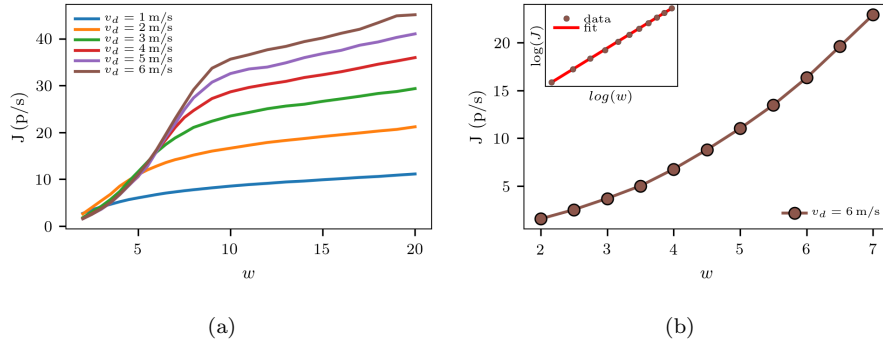


Figure B.11: **(a)** Evacuation flow as a function of door width w for the no-vestibule scenario. See the legend for the desired velocities explored. The initial crowd size is $N=200$. Data was averaged over 30 evacuation processes where the initial positions and velocities were random. The simulation finished when 180 pedestrians left the room. **(b)** Results corresponding to $v_d = 6$ m/s. The inset shows the linear regression applied to the $\log(J)$ and $\log(w)$. The regression is defined as $\log(J) = m \cdot \log(w) + b$. The slope value obtained from the linear fit is $m = 2.1$.

In order to have a deeper understanding of the phenomena. We calculated a linear regression to the log data from Fig. B.11b (see the inset plot). The slope obtained by this regression is $m = 2.1$. This means that the flow vs. w relation holds a quasi-quadratic behavior.

Although the analogy with granular media accelerated by gravity is not straightforward, we cannot fail to mention that there is an apparent similarity between the behavior described above and the Hagen-Beverloo's equation for the flow discharge of particles in a silo [37].

Appendix C. Types of Blocking clusters

In this appendix, we illustrate the blocking clusters that can be formed in the 2-doors vestibule layout. Three types of blocking clusters (BC) can be distinguished. The “exit door blocking cluster”, the “inside vestibule blocking cluster” (which is formed perpendicular to the vestibule length), and the “vestibule door blocking cluster”. This latter type of BC is formed in the zone prior to the vestibule door.

Acknowledgments

This work was supported by the Fondo para la investigación científica y tecnológica (FONCYT) grant Proyecto de investigación científica y tecnológica Number PICT-2019-2019-01994. G.A. Frank thanks Universidad Tecnológica Nacional (UTN) for partial support through Grant PID Number SIUTNBA0006595.

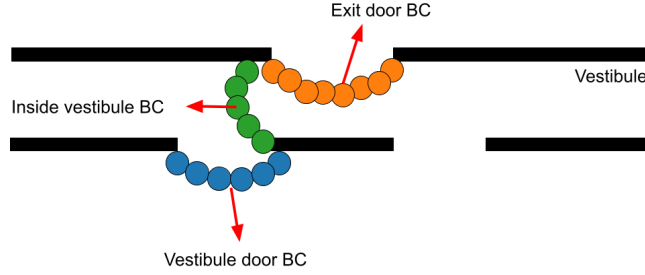


Figure C.12: Picture of the blocking clusters in the 2-doors vestibule layout. Each blocking cluster type has a unique color (orange, green, and blue). The colors are in accordance with the curves from Fig. 7. Those curves represent the blocking cluster probability as a function of the vestibule door width w .

References

References

- [1] D. T. G. Daniel, E. A. Alpert, E. Jaffe, The crowd crush at mount meron: Emergency medical services response to a silent mass casualty incident, *Disaster Medicine and Public Health Preparedness* (2022) 1–3.
- [2] M. M. de Almeida, J. von Schreeb, Human stampedes: An updated review of current literature, *Prehospital and disaster medicine* 34 (1) (2019) 82–88.
- [3] D. Helbing, I. Farkas, T. Vicsek, Simulating dynamical features of escape panic, *Nature* 407 (6803) (2000) 487–490.
- [4] A. Kirchner, K. Nishinari, A. Schadschneider, Friction effects and clogging in a cellular automaton model for pedestrian dynamics, *Physical review E* 67 (5) (2003) 056122.
- [5] M. Haghani, Optimising crowd evacuations: Mathematical, architectural and behavioural approaches, *Safety science* 128 (2020) 104745.
- [6] A. Abdelghany, K. Abdelghany, H. Mahmassani, W. Alhalabi, Modeling

- framework for optimal evacuation of large-scale crowded pedestrian facilities, *European Journal of Operational Research* 237 (3) (2014) 1105–1118.
- [7] S. C. Pursals, F. G. Garzón, Optimal building evacuation time considering evacuation routes, *European Journal of Operational Research* 192 (2) (2009) 692–699.
 - [8] X. Song, L. Ma, Y. Ma, C. Yang, H. Ji, Selfishness-and selflessness-based models of pedestrian room evacuation, *Physica A: Statistical Mechanics and its Applications* 447 (2016) 455–466.
 - [9] Y. Cheng, X. Zheng, Emergence of cooperation during an emergency evacuation, *Applied Mathematics and Computation* 320 (2018) 485–494.
 - [10] X. Shi, Z. Ye, N. Shiwakoti, D. Tang, J. Lin, Examining effect of architectural adjustment on pedestrian crowd flow at bottleneck, *Physica A: Statistical Mechanics and its Applications* 522 (2019) 350–364.
 - [11] D. Helbing, L. Buzna, A. Johansson, T. Werner, Self-organized pedestrian crowd dynamics: Experiments, simulations, and design solutions, *Transportation science* 39 (1) (2005) 1–24.
 - [12] G. A. Frank, C. O. Dorso, Room evacuation in the presence of an obstacle, *Physica A: Statistical Mechanics and its Applications* 390 (11) (2011) 2135–2145.
 - [13] I. Sticco, G. Frank, C. Dorso, Improving competitive evacuations with a vestibule structure designed from panel-like obstacles in the framework of the social force model, *Safety science* 146 (2022) 105544.
 - [14] Y. Zhao, T. Lu, L. Fu, P. Wu, M. Li, Experimental verification of escape efficiency enhancement by the presence of obstacles, *Safety science* 122 (2020) 104517.
 - [15] Á. Garcimartín, D. Maza, J. M. Pastor, D. R. Parisi, C. Martín-Gómez, I. Zuriguel, Redefining the role of obstacles in pedestrian evacuation, *New Journal of Physics* 20 (12) (2018) 123025.

- [16] C. Feliciani, I. Zuriguel, A. Garcimartín, D. Maza, K. Nishinari, Systematic experimental investigation of the obstacle effect during non-competitive and extremely competitive evacuations, *Scientific reports* 10 (1) (2020) 1–20.
- [17] D. Helbing, A. Johansson, H. Z. Al-Abideen, Dynamics of crowd disasters: An empirical study, *Physical review E* 75 (4) (2007) 046109.
- [18] A. Garcimartín, J. M. Pastor, C. Martín-Gómez, D. Parisi, I. Zuriguel, Pedestrian collective motion in competitive room evacuation, *Scientific reports* 7 (1) (2017) 1–9.
- [19] F. E. Cornes, G. A. Frank, C. O. Dorso, High pressures in room evacuation processes and a first approach to the dynamics around unconscious pedestrians, *Physica A: Statistical Mechanics and its Applications* 484 (2017) 282–298.
- [20] C. Wang, W. Weng, Study on the collision dynamics and the transmission pattern between pedestrians along the queue, *Journal of Statistical Mechanics: Theory and Experiment* 2018 (7) (2018) 073406.
- [21] G. H. Risto, H. J. Herrmann, et al., Density patterns in two-dimensional hoppers, *Physical Review E* 50 (1) (1994) R5.
- [22] I. Sticco, G. Frank, C. Dorso, Social force model parameter testing and optimization using a high stress real-life situation, *Physica A: Statistical Mechanics and its Applications* 561 (2021) 125299.
- [23] A. Strachan, C. Dorso, Fragment recognition in molecular dynamics, *Physical Review C* 56 (2) (1997) 995.
- [24] D. R. Parisi, C. O. Dorso, Microscopic dynamics of pedestrian evacuation, *Physica A: Statistical Mechanics and its Applications* 354 (2005) 606–618.
- [25] I. M. Sticco, G. A. Frank, S. Cerrotta, C. O. Dorso, Room evacuation through two contiguous exits, *Physica A: Statistical Mechanics and its Applications* 474 (2017) 172–185.

- [26] F. Cornes, G. Frank, C. Dorso, Microscopic dynamics of the evacuation phenomena in the context of the social force model, *Physica A: Statistical Mechanics and its Applications* 125744.
- [27] D. Littlefield, *Metric handbook*, Routledge, 2008.
- [28] D. R. Parisi, A. G. Sartorio, J. R. Colonnello, A. Garcimartín, L. A. Pugnaroni, I. Zuriguel, Pedestrian dynamics at the running of the bulls evidence an inaccessible region in the fundamental diagram, *Proceedings of the National Academy of Sciences* 118 (50) (2021) e2107827118.
- [29] S. Plimpton, Fast parallel algorithms for short-range molecular dynamics, *Journal of computational physics* 117 (1) (1995) 1–19.
- [30] C. M. Harris, *Dictionary of Architecture and Construction.*, McGraw-Hill, 2006.
- [31] Z. Ding, Z. Shen, N. Guo, K. Zhu, J. Long, Evacuation through area with obstacle that can be stepped over: experimental study, *Journal of Statistical Mechanics: Theory and Experiment* 2020 (2) (2020) 023404.
- [32] L. Fullard, E. Breard, C. Davies, A. Godfrey, M. Fukuoka, A. Wade, J. Dufek, G. Lube, The dynamics of granular flow from a silo with two symmetric openings, *Proceedings of the Royal Society A* 475 (2221) (2019) 20180462.
- [33] M. Haghani, M. Sarvi, Z. Shahhoseini, When ‘push’ does not come to ‘shove’: Revisiting ‘faster is slower’ in collective egress of human crowds, *Transportation research part A: policy and practice* 122 (2019) 51–69.
- [34] S. Gwynne, E. Kuligowski, J. Kratchman, J. A. Milke, Questioning the linear relationship between doorway width and achievable flow rate, *Fire Safety Journal* 44 (1) (2009) 80–87.
- [35] A. Seyfried, O. Passon, B. Steffen, M. Boltes, T. Rupprecht, W. Klingsch, New insights into pedestrian flow through bottlenecks, *Transportation Science* 43 (3) (2009) 395–406.

- [36] W. Tian, W. Song, J. Ma, Z. Fang, A. Seyfried, J. Liddle, Experimental study of pedestrian behaviors in a corridor based on digital image processing, *Fire Safety Journal* 47 (2012) 8–15.
- [37] W. A. Beverloo, H. A. Leniger, J. Van de Velde, The flow of granular solids through orifices, *Chemical engineering science* 15 (3-4) (1961) 260–269.